1521-0111/12/8203-372–382$25.00
MOLECULAR PHARMACOLOGY
Copyright © 2012 The American Society for Pharmacology and Experimental Therapeutics
Mol Pharmacol 82:372–382, 2012

Vol. 82, No. 3
78006/3785527

Vm24, a Natural Immunosuppressive Peptide, Potently and Selectively Blocks Kv1.3 Potassium Channels of Human T Cells

Zoltan Varga, Georgina Gurrola-Briones, Ferenc Papp, Ricardo C. Rodríguez de la Vega, Gustavo Pedraza-Alva, Rajeev B. Tajhya, Rezso Gaspar, Luis Cardenas, Yvonne Rosenstein, Christine Beeton, Lourival D. Possani, and Gyorgy Panyi

Department of Biophysics and Cell Biology, Research Center for Molecular Medicine, University of Debrecen, Debrecen, Hungary (Z.V., F.P., R.G., G.P.); Departments of Molecular Medicine and Bioprocesses (G.G.-B., G.P.-A., Y.R., L.D.P.) and Molecular and Plant Biology (L.C.), Institute of Biotechnology, National Autonomous University of Mexico, Cuernavaca, Mexico; Ecology, Systematics, and Evolution Laboratory, University of Paris-South, Orsay, France (R.C.R.V.); and Department of Molecular Physiology and Biophysics, Baylor College of Medicine, Houston, Texas (R.B.T., C.B.)

Received January 31, 2012; accepted May 23, 2012

ABSTRACT

Blockade of Kv1.3 K^+ channels in T cells is a promising therapeutic approach for the treatment of autoimmune diseases such as multiple sclerosis and type 1 diabetes mellitus. Vm24 (α-KTx 23.1) is a novel 36-residue Kv1.3-specific peptide isolated from the venom of the scorpion *Vaejovis mexicanus smithi*. Vm24 inhibits Kv1.3 channels of human lymphocytes with high affinity (K_d = 2.9 pM) and exhibits >1500-fold selectivity over other ion channels assayed. It inhibits the proliferation and Ca^{2+} signaling of human T cells in vitro and reduces delayed-type hypersensitivity reactions in rats in vivo. Our results indicate that Vm24 has exceptional pharmacological properties that make it an excellent candidate for treatment of certain autoimmune diseases.

Introduction

Autoimmune diseases are characterized by the generation of T-cell clones that react to self-antigens, which leads to the destruction of specific tissues such as myelinated neurons in multiple sclerosis or insulin-producing pancreatic β-cells in type 1 diabetes mellitus (Beeton et al., 2006). In these diseases, specific inhibition of the proliferation of autoreactive T cells mediating tissue damage [effector memory T (T_{EM}) cells] is desirable (Wulff et al., 2003).

An increase in the cytosolic free Ca^{2+} concentration ($[Ca^{2+}]_i$) is a key signal leading to T-cell proliferation (Lewis, 2001; Cahalan and Chandy, 2009). The membrane potential of T cells, which is sustained by the activity of voltage-gated, depolarization-activated Kv1.3 and Ca^{2+}-activated KCa3.1 K^+ channels, contributes to the electrochemical driving force for Ca^{2+} entry into the cells through plasma membrane Ca^{2+} release-activated Ca^{2+} channels (Leonard et al., 1992; Lin et al., 1993). Ca^{2+} release-activated Ca^{2+} channels assemble upon T-cell activation and subsequent intracellular Ca^{2+} store depletion, with STIM1 sensing the depletion of endoplasmic reticulum Ca^{2+} and Orai1 being the pore unit of the channel (Cahalan and Chandy, 2009). The activity of the K^+ channels provides the counterbalancing cation efflux required for maintenance of the negative membrane potential during Ca^{2+} influx. Inhibition of Kv1.3 and KCa3.1 depolarizes the membrane potential and inhibits Ca^{2+} entry, leading

This work was supported by the National Institutes of Health National Institute of Neurological Disorders and Stroke [Grant NS073712]; the Hungarian Scientific Research Fund [Grants K 60740, NK 61412]; the Hungarian Social Renewal Operational Program [Grants TÁMOP-4.2.2-08/1/2008-0019, TÁMOP-4.2.1/B-09/1/KONV-2010-007, TÁMOP-4.2.2-A-11/1/KONV-2012-0025], General Management of Academic Personnel Matters, National Autonomous University of Mexico [Grant IN204110]; the National Council for Science and Technology of Mexico; the Hungarian Science and Technology Foundation [Grant MX-10/207], and the European Union Seventh Framework Program [Grant 246556] (to R.C.R.V.). Z.V. is a Bolyai Fellow.

Article, publication date, and citation information can be found at http://molpharm.aspetjournals.org.

http://dx.doi.org/10.1124/mol.112.078006.

ABBREVIATIONS: T_{EM}, effector memory T; $[Ca^{2+}]_i$, cytosolic free Ca^{2+} concentration; CFSE, carboxyfluorescein succinimidyl ester; FACS, fluorescence-activated cell sorting; RCF, remaining current fraction; GFP, green fluorescent protein; DTH, delayed-type hypersensitivity; PBS, phosphate-buffered saline; ShK, *Stichodactyla helianthus* toxin; OSK1, *Orthochirus scrobiculosus* toxin 1; BmKTx, potassium blocking toxin from *Buthus martensi*; HgTx1, hongotoxin1; MgTx, margatoxin; HsTx1, *Heterometrus spinifer* toxin; ChTx, charybdotoxin; mAb, monoclonal antibody; h, human; m, mouse; r, rat.

to reduced T-cell proliferation (Panyi et al., 2004; Cahalan and Chandy, 2009).

T-cell subtype-specific expression of K^+ channels significantly influences the potency of K^+ channel blockers to inhibit T-cell proliferation. Kv1.3 is the dominant K^+ channel of T_{EM} cells, and its inhibition causes persistent suppression of T_{EM} cell proliferation (Wulff et al., 2003). Other T-cell subsets escape the Kv1.3 blocker-mediated inhibition of proliferation through transcriptional up-regulation of KCa3.1 (Ghanshani et al., 2000). The unique dependence of T_{EM} cells on Kv1.3 for proliferation points to high-affinity Kv1.3 inhibitors as potential therapeutic immunosuppressants (Cahalan and Chandy, 2009). To avoid unwanted side effects mediated by the blockade of other voltage-gated K^+ channels, a very high selectivity for Kv1.3 is compelling for a therapeutically applied blocker (Panyi et al., 2006).

Animal toxins and small-molecule inhibitors have been reported to display high affinity for Kv1.3, and some of the toxins are selective for Kv1.3 over KCa3.1 (Panyi et al., 2006), including scorpion toxins (e.g., margatoxin, noxiustoxin, and kaliotoxin) and the ShK toxin isolated from sea anemone. However, ion channels important for neuronal and muscle excitability are also inhibited by these toxins, with comparable affinities. For example, Kv1.1 is blocked by ShK (Kalman et al., 1998), whereas Kv1.2 is inhibited by margatoxin (Koch et al., 1997). Several successful attempts were made to engineer toxin variants with improved selectivity for Kv1.3. In the case of OSK1 and BmKTx, this was accomplished by introducing substitutions for natural amino acids in key positions, such as [Lys16,Asp20]-OSK1 (Mouhat et al., 2005) and [Arg11,Thr28,His33]-BmKTx (Han et al., 2008), which resulted in more than 100-fold selectivity for Kv1.3 while maintaining (OSK1 mutant) or increasing (BmKTx mutant) the affinity for Kv1.3. ShK mutants containing a non-natural amino acid (e.g., ShK-Dap22) or various N-terminal modifications (e.g., ShK-192) (Pennington et al., 2009) also exhibited distinctive selectivity and affinity for Kv1.3.

We describe here the exceptional pharmacological properties of Vm24, a natural peptide that was identified as part of the proteomic analysis of venom collected from the Mexican scorpion *Vaejovis mexicanus smithi*. Vm24, the first member of a novel αKTx subfamily, is a 36-residue peptide cross-linked by eight cysteines, which form a distorted cysteine-stabilized α/β motif (details provided by Gurrola et al., 2012). Although Vm24 shares structural similarities with other K^+ channel blockers, including an α-helix and β-turns with a diad-like arrangement of Lys25 and Tyr34 (Dauplais et al., 1997), it shows less than 50% identity with respect to other known αKTx peptides. In this study, we investigated whether the unique primary structure of Vm24 is reflected in its pharmacological properties. Vm24 blocked Kv1.3 channels with very high affinity (K_d = 2.9 pM) and with more than 1500-fold selectivity against a panel of channels used in this study (hKv1.3 $\gg$ hKv1.2 $>$ hKCa3.1 $>$ mKv1.1 $\gg$ hKv1.4 $\approx$ hKv1.5 $\approx$ rKv2.1 $\approx$ hKv11.1 $\approx$ hKCa1.1 $\approx$ hKCa2.3 $\approx$ hNa$_v$1.5). Vm24 inhibited Ca^{2+} signaling in human T lymphocytes at concentrations that blocked Kv1.3 and in vitro T-cell proliferation and effectively reduced delayed-type hypersensitivity (DTH) in rats. The unique affinity and selectivity of the natural peptide for Kv1.3 makes Vm24 an excellent candidate for Kv1.3 blockade-mediated treatment of certain autoimmune diseases, such as multiple sclerosis, rheumatoid arthritis, and type 1 diabetes.

Materials and Methods

Isolation and Sequence Determination of Vm24. A detailed description of the procedures for venom preparation, purification, proteomic analysis, sequencing, and three-dimensional NMR structure determination, as well as phylogenetic tree analysis and molecular modeling of the interaction of Vm24 with K^+ channels, was reported previously (Gurrola et al., 2012). The soluble venom of *V. mexicanus smithi* was separated with high-performance liquid chromatography, and each component was collected separately and immediately freeze-dried. The molecular mass of each subfraction was evaluated through mass spectrometry, using equipment and procedures described previously (Batista et al., 2007). Fractions containing molecular masses in the range expected for K^+ channel blockers (~4000 Da) were selected for electrophysiological assays. Among these fractions was one that eluted at 24 min, which was further separated; this separation produced a homogeneous peptide with a molecular mass of 3864 Da, which was named Vm24. Because this component was shown to be a potent inhibitor of Kv1.3 channels, its full amino acid sequence was determined. Direct sequence analysis was performed through automatic Edman degradation, and results were confirmed with mass spectrometry. Initial sequencing results for Vm24 yielded unequivocal amino acid sequence data for the first 23 amino acid residues. Two peptides obtained through endopeptidase Arg-C1 cleavage allowed identification of the sequences from Ala18 to Arg29 and from Lys30 to Cys36. Overlap information was obtained with two additional peptides, one obtained through tryptic digestion that allowed identification of residues from Cys26 to Lys32 and a confirmatory peptide obtained through Lys-C digestion that corresponded to the sequence from Cys33 to Cys36 (Gurrola et al., 2012). The full sequence obtained was AAAISCVGSPECPPKCRAQGCKNGKCMNRKCKCY-YC-amide (Gurrola et al., 2012).

Human T Lymphocytes for Patch-Clamp Recordings. Heparinized human peripheral venous blood was obtained from healthy volunteers. Mononuclear cells were separated through Histopaque-1077 (Sigma-Aldrich Hungary, Budapest, Hungary) density gradient centrifugation. Collected cells were washed twice with Ca^{2+}- and Mg^{2+}-free Hanks' solution containing 25 mM HEPES buffer, pH 7.4. Cells were cultured for 3 to 4 days in 24-well culture plates in a 5% CO_2 incubator at 37°C, in RPMI 1640 medium supplemented with 10% fetal calf serum (Sigma-Aldrich), 100 μg/ml penicillin, 100 μg/ml streptomycin, and 2 mM L-glutamine (density, 0.5×10^6 cells per ml). The culture medium also contained 6 or 8 μg/ml phytohemagglutinin A (Sigma-Aldrich), to increase K^+ channel expression. T lymphocytes were selected for recording of hKv1.3 currents through incubation with mouse anti-human CD2 (BD Biosciences, San Jose, CA), followed by selective adhesion to Petri dishes coated with goat anti-mouse IgG antibodies (BioSource International, Camarillo, CA), as described previously (Matteson and Deutsch, 1984). Dishes were washed gently five times with 1 ml of normal extracellular bath medium (see below) for the patch-clamp experiments.

Human T Cells for Proliferation Assays. The buffy coat containing mononuclear cells was resuspended in RPMI 1640 medium supplemented with 5% fetal calf serum, 2 mM L-glutamine (Sigma-Aldrich), 50 units/ml penicillin, 50 μg/ml streptomycin, and 50 mM β-mercaptoethanol, and the cells were plated onto 100-mm Petri dishes (8×10^7 cells per plate) and incubated overnight at 37°C in 5% CO_2. Before experimentation, nonadherent cells (peripheral blood mononuclear cells) were cultured for 24 h at 37°C in 5% CO_2, in RPMI 1640 medium supplemented with 2% fetal calf serum.

Activation of T Cells for Proliferation Assays. Cells were stimulated with anti-CD3 (OKT3, 100 ng/ml; American Type Culture Collection, Manassas, VA) and anti-CD28 (500 ng/ml; Ancell Corp., Bayport, MN) mAbs at room temperature for 15 min, after which a secondary anti-mouse polyclonal antibody (rabbit anti-mouse immu-

noglobulin, 1 μg/ml) was added to cross-link the primary antibodies (Fierro et al., 2006). Cells were then incubated at 37°C in 5% CO_2 for the indicated times. CD25 expression was evaluated 24 h after stimulation, and cell proliferation was assessed through CFSE dilution 96 h after stimulation. Before activation, peripheral blood mononuclear cells (3–10 × 10^6 cells per ml) were labeled with CFSE (0.5 μM; Invitrogen, Carlsbad, CA) for 10 min at 37°C in the dark, washed with supplemented RPMI 1640 medium to eliminate excess dye, and placed under culture conditions, as described previously (Muul et al., 2008). Vm24, at various concentrations, was added at the onset of stimulation or 30 min before stimulation.

FACS Staining and Analysis. Cells (1 × 10^6) were resuspended in 100 μl of phosphate-buffered saline containing 2% fetal calf serum and 1% sodium azide (FACS solution) and were incubated with phycoerythrin-labeled anti-CD25 (Invitrogen) and tricolor-conjugated anti-CD3 (Invitrogen) for 30 min at 4°C. Cells were then washed with FACS solution through centrifugation at 300*g* and were fixed in 1% paraformaldehyde. Cells were sorted with a FACSort system with CellQuest (BD Biosciences) and were analyzed with FlowJo (Tree Star Inc., Ashland, OR), with gating on the $CD3^+$ population.

Cells for Heterologous Expression of Ion Channels. COS-7, human embryonic kidney 293, tsA201, L929, and MEL cells were grown under standard conditions, as described previously (Grissmer et al., 1994; Bagdány et al., 2005; Corzo et al., 2008).

Expression of Recombinant Ion Channels. COS-7 cells were used to express rKv2.1 (a kind gift from Dr. S. Korn, University of Connecticut, Storrs, CT), hKv1.2 (pcDNA3/Hygro vector containing the full coding sequence for Kv1.2; a kind gift from Dr. S. Grissmer, Ulm University, Ulm, Germany), hKv1.4 (hKv1.4-IR, the inactivation ball deletion mutant of Kv1.4; a kind gift from D. Fedida, University of British Columbia, Vancouver, Canada), and hKCa3.1 (*hIKCa1* gene, GenBank accession no. AF033021) and hKCa2.3 (*hSKCa3* gene), both in the pEGFP-C1 vector (Wulff et al., 2001) (kind gifts from Dr. Heike Wulff, University of California, Davis, CA). These channel clones were transiently cotransfected with a plasmid encoding the green fluorescent protein (GFP) (except hKCa3.1 and hKCa2.3, which were used in an enhanced GFP vector), at molar ratios of 1:5, by using Lipofectamine 2000 (Invitrogen) according to the manufacturer's protocol and were cultured under standard conditions. Currents were recorded 24 h after transfection. GFP-positive transfectants were identified with a Nikon TE2000U fluorescence microscope (Nikon, Tokyo, Japan) and were used for current recordings (>70% success rate for cotransfection).

The tsA201 cells were used to express hNav1.5 (a gift from R. Horn, Thomas Jefferson University, Philadelphia, PA) and hKCa1.1 (*hSlo1* gene in pCI-neo plasmid, GenBank accession no. U11058; a gift from T. Hoshi, University of Pennsylvania, Philadelphia, PA). L929 cells stably expressing mKv1.1 channels and MEL cells stably expressing hKv1.5 channels were described previously (Grissmer et al., 1994) and were gifts from Dr. Heike Wulff. hKv11.1 (*hERG*) channels were expressed in a stable manner in human embryonic kidney 293 cells.

Electrophysiological Studies. Whole-cell currents were measured in voltage-clamped cells according to standard protocols (Péter et al., 2001; Bagdány et al., 2005; Corzo et al., 2008), by using Axopatch 200A and Multiclamp 700B amplifiers connected to a personal computer with Axon Digidata 1200 and 1322A data acquisition hardware, respectively (Molecular Devices, Sunnyvale, CA). Series resistance compensation up to 70% was used to minimize voltage errors and to achieve good voltage-clamp conditions. Cells were observed with Nikon TE2000-U or Leitz Fluovert (Leica, Wetzlar, Germany) fluorescence microscopes, by using band-pass filters of 455 to 495 nm and 515 to 555 nm for excitation and emission, respectively. Cells displaying strong fluorescence were selected for current recordings, and >70% of those cells displayed cotransfected current. Pipettes were pulled from GC 150 F-15 borosilicate glass capillaries Harvard Apparatus (Kent, UK) in five stages and fire-polished, which resulted in electrodes having 3- to 5-MΩ resistance in the bath. For measurements of most channels, the bath solution consisted of 145 mM NaCl, 5 mM KCl, 1 mM $MgCl_2$, 2.5 mM $CaCl_2$, 5.5 mM glucose, and 10 mM HEPES, pH 7.35, supplemented with 0.1 mg/ml bovine serum albumin (Sigma-Aldrich). For recordings of hKv11.1 (hERG) currents, the bath solution contained 140 mM choline chloride, 5 mM KCl, 2 mM $MgCl_2$, 2 mM $CaCl_2$, 0.1 mM $CdCl_2$, 20 mM glucose, and 10 mM HEPES (pH 7.35). The measured osmolarity of the external solutions was between 302 and 308 mOsM. The internal solution contained 140 mM KF, 2 mM $MgCl_2$, 1 mM $CaCl_2$, 10 mM HEPES, and 11 mM EGTA (pH 7.22). For recordings of hKCa1.1 (hBK) currents, the composition of the pipette filling solution was 140 mM KCl, 10 mM EGTA, 9.69 mM $CaCl_2$, 5 mM HEPES, pH 7.2. The free Ca^{2+} concentration of the latter solution was 5 μM, which allowed recording of hKCa1.1 currents at moderately depolarizing potentials (Avdonin et al., 2003). For recordings of KCa3.1 and KCa2.3 currents, the composition of the pipette filling solution was 150 mM potassium aspartate, 5 mM HEPES, 10 mM EGTA, 8.7 mM $CaCl_2$, 2 mM $MgCl_2$, pH 7.2. This solution contained 1 μM free Ca^{2+}, to activate the KCa3.1 current fully (Grissmer et al., 1993). For recordings of Kv11.1 currents, the pipette solution contained 140 mM KCl, 10 mM EGTA, 2 mM $MgCl_2$, and 10 mM HEPES, pH 7.3. The measured osmolarity of the internal solutions was approximately 295 mOsM. Bath perfusion around the measured cell with different test solutions was achieved by using a gravity-flow perfusion system. Excess fluid was removed continuously.

For measurements of currents from mKv1.1, hKv1.2, hKv1.3, fast inactivation-removed hKv1.4 (Kv1.4ΔN), hKv1.5, and rKv2.1 channels, voltage steps to +50 mV were applied from a holding potential of −120 mV every 15 or 30 s. For hKv11.1 (hERG) channels, currents were evoked with a voltage step to +20 mV followed by a step to −40 mV, during which the peak current was measured. The holding potential was −80 mV, and pulses were delivered every 30 s. For KCa1.1 channels, a voltage step to +50 mV was preceded by a 10-ms hyperpolarization to −120 mV from a holding potential of 0 mV. Pulses were delivered every 5 s. Currents through Ca^{2+}-activated K^+ channels of T lymphocytes (hKCa3.1 or hIKCa1) were elicited every 10 s with voltage ramps to +50 mV from a holding potential of −120 mV. A similar protocol was used to measure human KCa2.3 currents, except that the voltage ramps were started from a holding potential of −100 mV. Currents through Nav1.5 channels were evoked every 15 s with voltage steps to 0 mV from a holding potential of −120 mV.

For data acquisition and analysis, the pClamp8/10 software package (Molecular Devices) was used. In general, currents were low-pass-filtered by using the built-in analog four-pole Bessel filters of the amplifiers and were sampled (2–50 kHz) at at least twice the filter cut-off frequency. Before analysis, whole-cell current traces were corrected for ohmic leakage and were digitally filtered (three-point boxcar smoothing). Each data point of the concentration-response curves represents the mean of three to seven independent experiments, and error bars represent the S.E.M. Data points were fitted with a two-parameter Hill equation, $RCF = K_d^n/(K_d^n + [Tx]^n)$, where RCF is the remaining current fraction ($RCF = I/I_0$, where I and I_0 are current amplitudes in the presence and absence, respectively, of toxin at a given concentration), K_d is the dissociation constant, n is the Hill coefficient, and [Tx] is the toxin concentration. Where indicated, K_d was estimated from the RCF value obtained with a single toxin concentration and $n = 1$ was used for the Hill equation.

Because of the extremely slow blocking kinetics for the current, we could not determine equilibrium block with low picomolar concentrations of Vm24; block equilibrium would require 0.5 to 1 h of toxin application to develop. Under these conditions, the decrease in the peak current from episode to episode was so small that apparent saturation was observed during data collection, although the block might not have reached its equilibrium value. During extended periods of toxin application, significant rundown of whole-cell currents may occur. Rundown of the peak currents could not be determined

independently because of the extremely long washout kinetics for the peptide. These factors indicated the use of an operational definition of equilibrium block as the peak current at which consecutive pulses in the presence of toxin caused negligible current decreases (less than 2%). This means that, in the RCF = I/I_0 equation, I is overestimated; therefore, the K_d value determined from the dose-response curve is also overestimated.

Measurements of Intracellular Ca^{2+} Concentrations. Human peripheral T cells were loaded with 1 μM Fura2/acetoxymethyl ester (Invitrogen) for 30 min at 37°C and were plated in poly-L-lysine-coated LabTek chambers (Nalge Nunc International, Rochester, NY) at 1.5×10^6 cells per ml, in the absence or presence of 10 nM Vm24, 30 min before activation. Under a fluorescence microscope, T cells were incubated with 100 ng/ml anti-CD3 mAb and 500 ng/ml anti-CD28 mAb for 2 min before cross-linking of anti-CD3 and anti-CD28 mAbs with 1 μg/ml rabbit anti-mouse IgG. Finally, cells were treated with 5 mM levels of the calcium ionophore ionomycin. The changes in intracellular Ca^{2+} levels were analyzed with MetaMorph/MetaFluor software (Molecular Devices).

In Vivo DTH Reactions. All animal trials were approved by the Baylor College of Medicine institutional animal use and care committee. Female Lewis rats (9–10 weeks of age) were purchased from Harlan (Indianapolis, IN) and were housed under pathogen-free conditions, with food and water available ad libitum.

Active DTH was induced as described previously (Beeton and Chandy, 2007a), by immunizing rats against ovalbumin emulsified with complete Freund's adjuvant (Sigma-Aldrich). Animals were challenged 7 days later with ovalbumin (20 μg in 20 μl of saline solution) in the pinna of one ear (challenged ear). The other ear received saline solution (challenge control). Rats received a single subcutaneous injection of either vehicle (PBS plus 2% rat serum) or 0.1 mg/kg Vm24 in 0.5 ml of vehicle, in the scruff of the neck, at the time of challenge.

Adoptive DTH was induced as described previously (Beeton and Chandy, 2007b), through intraperitoneal injection of in vitro-activated Ova-GFP T lymphocytes (5×10^6 cells per rat; a kind gift from Dr. Flügel, University of Goettingen, Goettingen, Germany) in 1 ml of saline solution. Rats were challenged in the ear and received Vm24 or vehicle 2 days later, as described above.

In both DTH analyses, ear thickness was measured 24 h after the challenge, by using a spring-loaded micrometer (Mitutoyo, Aurora, IL) with three-digit precision. The means of six measurements at the same point were calculated and used for statistical analyses. Specific ear swelling (change in ear thickness) was calculated as follows: challenged (ovalbumin-treated) ear thickness minus challenge control (PBS-treated) ear thickness.

Results

Vm24 Is a High-Affinity Blocker of Kv1.3 Channels. The standard voltage protocol used to evoke voltage-gated, Kv1.3-mediated, K^+ currents in T cells consisted of a series of 14-ms depolarizations to +50 mV from a holding potential of −120 mV. The time between voltage pulses was set to 15 s, to avoid cumulative inactivation of hKv1.3 channels. Representative current traces in normal bath solution are shown in Fig. 1A. Under the experimental conditions detailed in *Materials and Methods* and in the legend to Fig. 1 (the lack of Ca^{2+} in the pipette filling solution and the voltage protocol used), hKv1.3 channels are exclusively responsible for the whole-cell currents (Péter et al., 2001). Figure 1A displays macroscopic K^+ currents through hKv1.3 channels recorded sequentially in the same cell, before (control traces) and after the addition of 1 nM Vm24 to the external solution through perfusion. The Kv1.3 current completely disappeared by the 12th pulse (corresponding to 3 min) in the presence of 1 nM Vm24. Washing the perfusion chamber with toxin-free solution for several minutes resulted in no significant amount of current recovery (data not shown).

The kinetic features of the development of current inhibition at 1 and 0.3 nM Vm24 are shown in Fig. 1B. After the fourth pulse in control solution, the extracellular perfusion solution was switched to a toxin-containing solution and the depolarizing pulses were continued every 15 s. Peak currents were determined and normalized to the peak current in con-

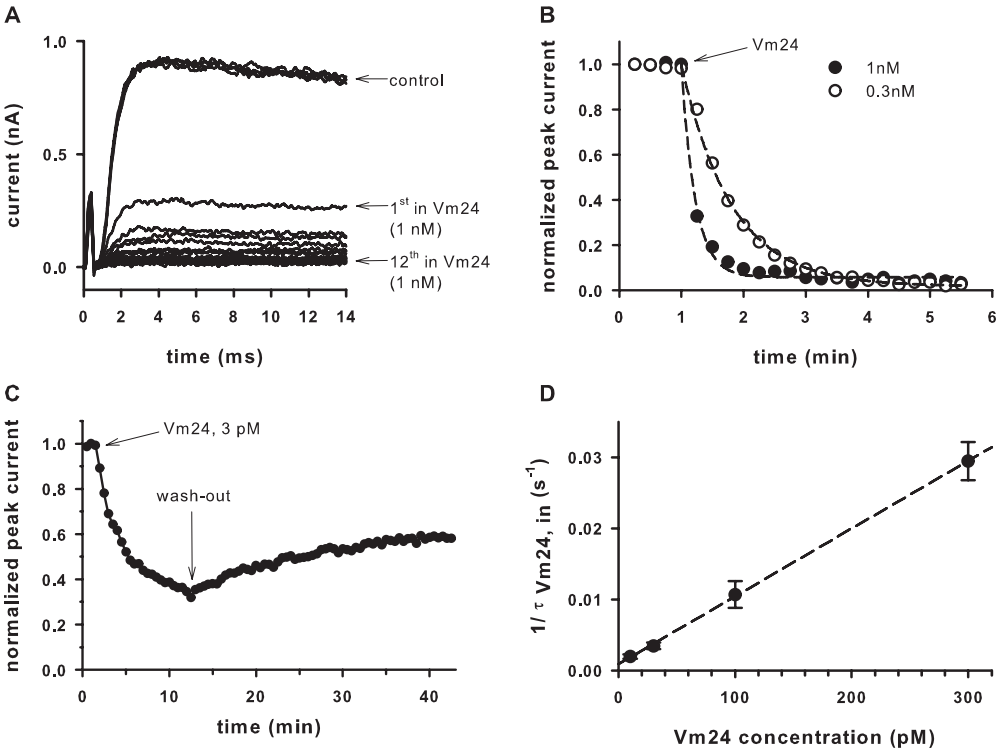

Fig. 1. Block of Kv1.3 channels by Vm24. A, whole-cell potassium currents through hKv1.3 channels evoked from a human T cell in response to depolarizing pulses to +50 mV from a holding potential of −120 mV every 15 s. Currents in the absence of Vm24 (control) were almost completely blocked when 1 nM Vm24 was administered to the cell through perfusion in the extracellular medium. Arrows indicate the first and 12th pulses with Vm24. B, normalized peak currents as a function of time after the application of 1 or 0.3 nM Vm24. The arrow indicates the start of the application of toxin. C, normalized peak currents of a lymphocyte as a function of time as 3 pM Vm24 was applied to the cell and then removed (wash-out) from the extracellular medium. Perfusion with toxin-free medium resulted in very slow partial recovery from block, with a time constant of ~3800 s. Pulses were delivered every 30 s. D, rate of block (inverse of $\tau_{Vm24,in}$) as a function of the Vm24 concentration. Data points were fitted with a linear function (r^2 = 0.99).

trol solution, and values were plotted as a function of time. At higher toxin concentrations, current inhibition was faster, as expected for a pseudo-first-order reaction between the toxin and the channels. At either concentration, the toxin totally inhibited the whole-cell Kv1.3 current. Perfusion of the recording chamber with toxin-free control solution resulted in a very small amount of blockade relief within the first 8 min (data not shown). During a 10.5-min period of application of the toxin at 3 pM (Fig. 1C), the loss of the current was apparently saturated at ~36% of the peak recorded in control solution. Toxin application was followed by a 30-min washout period, during which one third of the blocked current was recovered with extremely slow kinetics (the estimated time constant for washout was ~3800 s, corresponding to an off-rate of $\sim 2.63 \times 10^{-4}$ s^{-1}).

Figure 1D shows the analysis of kinetic features of the development of current inhibition at various Vm24 concentrations. The kinetics were characterized by fitting a single-exponential decay function to the normalized peak current-time relationships (Fig. 1B). With the assumption of a bimolecular reaction between the toxin and the channel, the resulting wash-in time constant ($\tau_{Vm24,in}$) was $1/((k_{on} \times [Vm24] + k_{off})$, where k_{on} and k_{off} are the molecular rate constants of toxin association to and dissociation from the channel and [Vm24] is the peptide concentration. Because of the extremely slow wash-out kinetics and consequently the negligible value of k_{off} ($k_{off} = 1/\tau_{out}$), the off-rate of the toxin was neglected at Vm24 concentrations of ≥10 pM and k_{on} was determined from the toxin concentration and the reciprocal of the wash-in time constant (i.e., $k_{on} \approx 1/([Vm24] \times \tau_{Vm24,in})$. Plotting of $1/\tau_{Vm24,in}$ values as a function of the Vm24 concentrations resulted in a linear relationship, with $k_{on} = 9.55 \times 10^7$ M^{-1} s^{-1} ($r^2 = 0.99$, linear regression) (Fig. 1D).

To prove that the inhibition of current by Vm24 was a consequence of blockade of Kv1.3 channels (similar to the action of other scorpion toxins), we designed competition experiments with Vm24 and charybdotoxin (ChTx). ChTx is a well characterized blocker of several K^+ channels that is known to occlude the pore by binding in the extracellular mouth of the channels (Goldstein and Miller, 1993). We determined $\tau_{Vm24,in}$ for 0.3 nM Vm24 in the absence of ChTx (Fig. 1) and in the presence of various concentrations of ChTx after equilibration of the block of Kv1.3 channels (Fig. 2). We chose 0.3 nM Vm24 for the competition experiments because it caused complete current inhibition with a kinetic profile that could be measured accurately with the minimum of 15-s intervals between successive current recordings. Figure 2A shows a representative experiment in which the current was blocked with 0.3 nM ChTx and then the perfusion solution was switched to an extracellular solution containing 0.3 nM Vm24 plus 0.3 nM ChTx. If the toxins competed for the same binding sites, then a slower blocking rate for Vm24 in the presence of ChTx would be expected, because only a fraction of the channels (determined on the basis of the ChTx concentration) would be available for block by Vm24. Figure 2B shows normalized peak currents recorded in different cells in the presence of only 0.3 nM Vm24 or in the presence of the two toxins simultaneously, after equilibration of the block by 0.3 or 2.5 nM ChTx. The reduction of the peak currents exhibited exponential decay in all cases, and the block rate was determined as $1/\tau_{in,Vm24}$ (see above). In Fig. 2C, $1/\tau_{in,Vm24}$ was plotted as a function of channels not blocked by

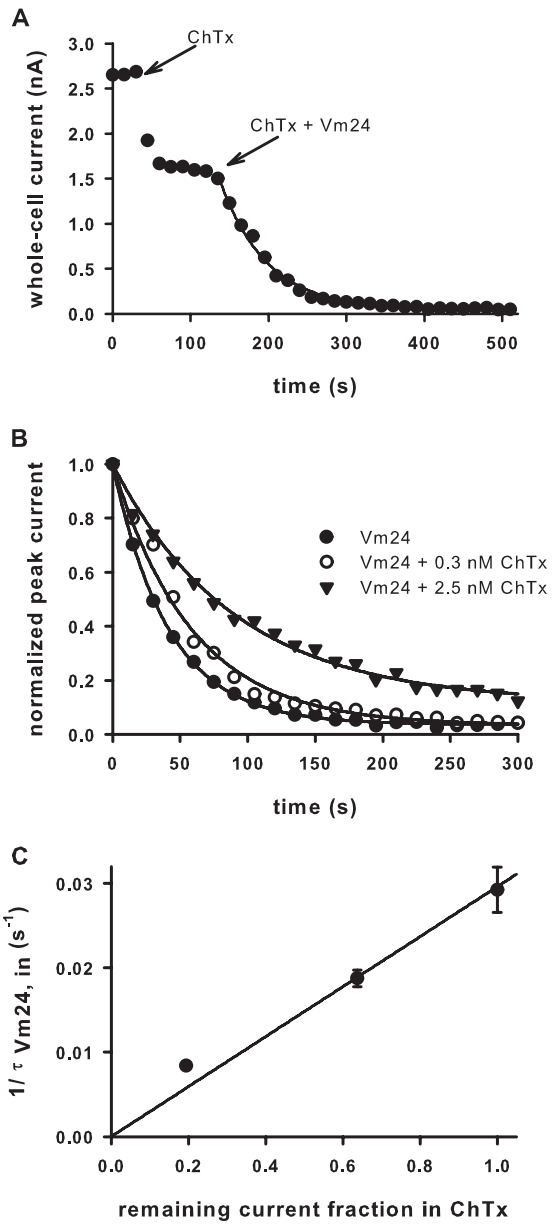

Fig. 2. Competition between ChTx and Vm24. A, peak whole-cell Kv1.3 currents of a human T cell exposed to 0.3 nM ChTx and, after equilibration of the block, to a mixture of 0.3 nM ChTx and 0.3 nM Vm24. Vm24 block kinetics were measured by fitting the peak currents with a single-exponential decay model and determining the time constant. B, normalized peak currents of human T cells, illustrating the kinetics of blockade produced by 0.3 nM Vm24 in the absence or presence of the indicated concentrations of ChTx. C, rate of blockade (inverse of the wash-in time constant) by 0.3 nM Vm24 as a function of the remaining current fraction (unblocked channel fraction) in the absence or presence of 0.3, 1, or 2.5 nM ChTx. Data points were fitted with a linear function ($r^2 = 0.967$).

ChTx; the latter term represents the RCF in the presence of only ChTx (RCF = I/I_0, where I and I_0 are the peak currents measured in the presence of the toxin after equilibration of the block and in the absence of the toxin, respectively). Figure 2C shows that $1/\tau_{in,Vm24}$ was directly proportional to RCF ($r^2 = 0.967$), as expected for two toxins competing for the same binding site.

To determine the dose dependence of current inhibition by Vm24, accurate measurements of equilibrium block at low picomolar concentrations required special analysis, because

of the very slow blocking kinetics. With the method detailed under *Materials and Methods*, RCF values were determined and plotted as a function of toxin concentrations. The dose-response relationship was obtained by fitting the data points with the Hill equation (Fig. 3), which yielded a dissociation constant of 2.9 pM and a Hill coefficient of ~1.

Vm24 Exhibits More than 1500-Fold Selectivity for Kv1.3 over KCa3.1, Kv1.1, and Kv1.2 and Does Not Inhibit a Wide Range of Other Channels. For a peptide to be an efficient immunosuppressant, it needs to be selective for Kv1.3 over other biologically relevant channels. As mentioned above, hKCa3.1 is notable in this respect, because it is expressed endogenously in T cells (Grissmer et al., 1993) and its expression levels vary among different T-cell subsets (Wulff et al., 2003). The potency of Vm24 to inhibit hKCa3.1 channels was assayed with channels expressed heterologously in COS-7 cells. Although human peripheral blood T cells also express hKCa3.1, we chose to use recombinant channels because the number of channels expressed could be increased sufficiently to allow accurate determination of the pharmacological properties of the channels in the absence of Kv1.3. Figure 4A shows that the voltage ramp applied evoked pure, non–voltage-gated, hKCa3.1 currents, and the change in the slope of the current could be used to characterize the current block (Grissmer et al., 1993).

In addition to hKCa3.1, we assayed the effects of Vm24 on the currents of the following eight K^+ channels and one human cardiac Na^+ channel: mKv1.1 (Fig. 4B), hKv1.2 (Fig. 4C), hKv1.4ΔN (fast inactivation-removed hKv1.4) (Fig. 4D), hKv1.5 (Fig. 4E), hKv2.1 (Fig. 4F), hKCa1.1 (Fig. 4G), hKCa2.3 (Fig. 4H), hKv11.1 (Fig. 4I), and hNav1.5 (Fig. 4J). Of the tested channels, hKCa3.1, mKv1.1, and hKv1.2 were partially blocked by the peptide at 10 nM, whereas the other channels were unaffected (Figs. 4 and 5A). This concentration was ~3500 times the K_d for hKv1.3 and resulted in RCF values of 0.59 ± 0.03, 0.80 ± 0.02, and 0.54 ± 0.08 for hKCa3.1, mKv1.1, and hKv1.2 channels, respectively (n = 3 for each channel) (Fig. 5A). The affected channels were also tested with 1 nM toxin, which yielded RCF values of 0.95 ± 0.02, 0.97 ± 0.02, and 0.81 ± 0.02, respectively (n = 3 for each channel) (Fig. 5, B and C). From the RCF values, the affinity of Vm24 for these channels could be estimated with a model in which one toxin molecule interacted with one channel, which yielded K_d values of 14 to 30 nM for KCa3.1, 30 to 40 nM for mKv1.1, and 5 to 10 nM for hKv1.2. These values were at least 4500, 10,000, and 1500 times higher, respectively, than the K_d for Kv1.3.

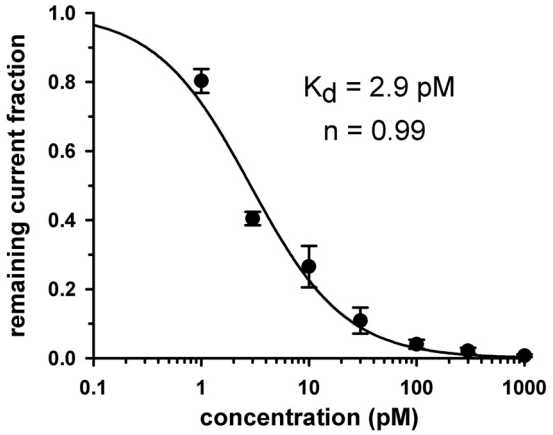

Fig. 3. Dose-response relationship for Vm24. The dose-response was obtained by plotting the remaining current fraction (RCF = I/I_0) as a function of toxin concentration (where I and I_0 are the peak currents measured in the presence and absence of toxin, respectively) and fitting the data points with the function RCF = $K_d^n/(K_d^n + [T_x]^n)$ (where [Tx] indicates the toxin concentration and K_d is the dissociation constant). Error bars indicate S.E.M. (n = 3–6). The dose-response function constructed in this way yielded a K_d of 2.9 pM and a Hill coefficient of ~1 (for details of determination of the equilibrium block, see *Materials and Methods*).

Vm24 Inhibits T Cell Proliferation, CD25 Expression, and Ca^{2+} Signaling In Vitro and Suppresses DTH Reactions In Vivo. High-affinity, specific blockers of Kv1.3 channels inhibit distinctively the proliferation of human T cells (Hu et al., 2007). We assessed whether CD3/CD28-dependent T-cell activation and proliferation were inhibited by Vm24. Freshly isolated, proliferation-arrested human T lymphocytes were stimulated with the combination of anti-CD3 and anti-CD28 antibodies (cross-linked with polyclonal anti-mouse IgG to maximize stimulation). The progression of the cell cycle (i.e., the number of cell divisions) was monitored by using the CFSE dilution assay. Figure 6A shows that preincubation of the cells with Vm24 before CD3-CD28 ligation resulted in a clear, dose-dependent reduction in the number of cells that proliferated after 96 h but did not limit the number of cell divisions for the cells that proliferated. The Vm24 concentrations that inhibited proliferation were comparable to those that inhibited Kv1.3 channels in electrophysiological assays, as shown by the overlap of the dose-response curves for the current block and proliferation inhibition (Fig. 6B). Simultaneous addition of the peptide and the stimulus yielded the same results (data not shown).

Upon T-cell activation, expression of the interleukin-2 receptor α-chain (CD25) is up-regulated. Moreover, CD25 expression was shown to parallel Kv1.3 activity in both $CD4^+$ and $CD8^+$ cells (Estes et al., 2008). On the basis of these findings, we tested whether Vm24 would interfere with the expression of CD25 in human T cells. Figure 6A, right, shows that addition of Vm24, 30 min before T-cell activation through CD3-CD28 ligation, decreased the number of T lymphocytes expressing CD25, in a dose-dependent manner. Therefore, the reduction in T-cell proliferation observed in the presence of Vm24 was in part attributable to a reduction in the expression of CD25 (Fig. 6B).

Because both T-cell proliferation and CD25 expression depend on the Ca^{2+} signal accompanying T-cell activation, we tested the influence of Vm24 on the CD3-CD28 ligation-induced increase in $[Ca^{2+}]_i$. T cells were incubated with Vm24 for 30 min before T-cell activation, and $[Ca^{2+}]_i$ was determined through microscopy. Figure 6C shows that 10 nM Vm24 abrogated the CD3-CD28-dependent Ca^{2+} mobilization but did not prevent the Ca^{2+} influx mediated by the calcium ionophore ionomycin. Together, these results suggest that the in vitro inhibition of proliferation and that of CD25 expression can be accounted for by the blocking of Kv1.3-mediated Ca^{2+} mobilization in human peripheral blood T lymphocytes.

We assessed the in vivo immunosuppressive capacity of Vm24 by determining its potency to inhibit active (Fig. 7A) or adoptive (Fig. 7B) DTH reactions. DTH is an example of a skin lesion caused by skin-homing T_{EM} cells (Soler et al., 2003). Active DTH was evoked with ovalbumin immunization and subsequent ovalbumin challenge, which resulted in

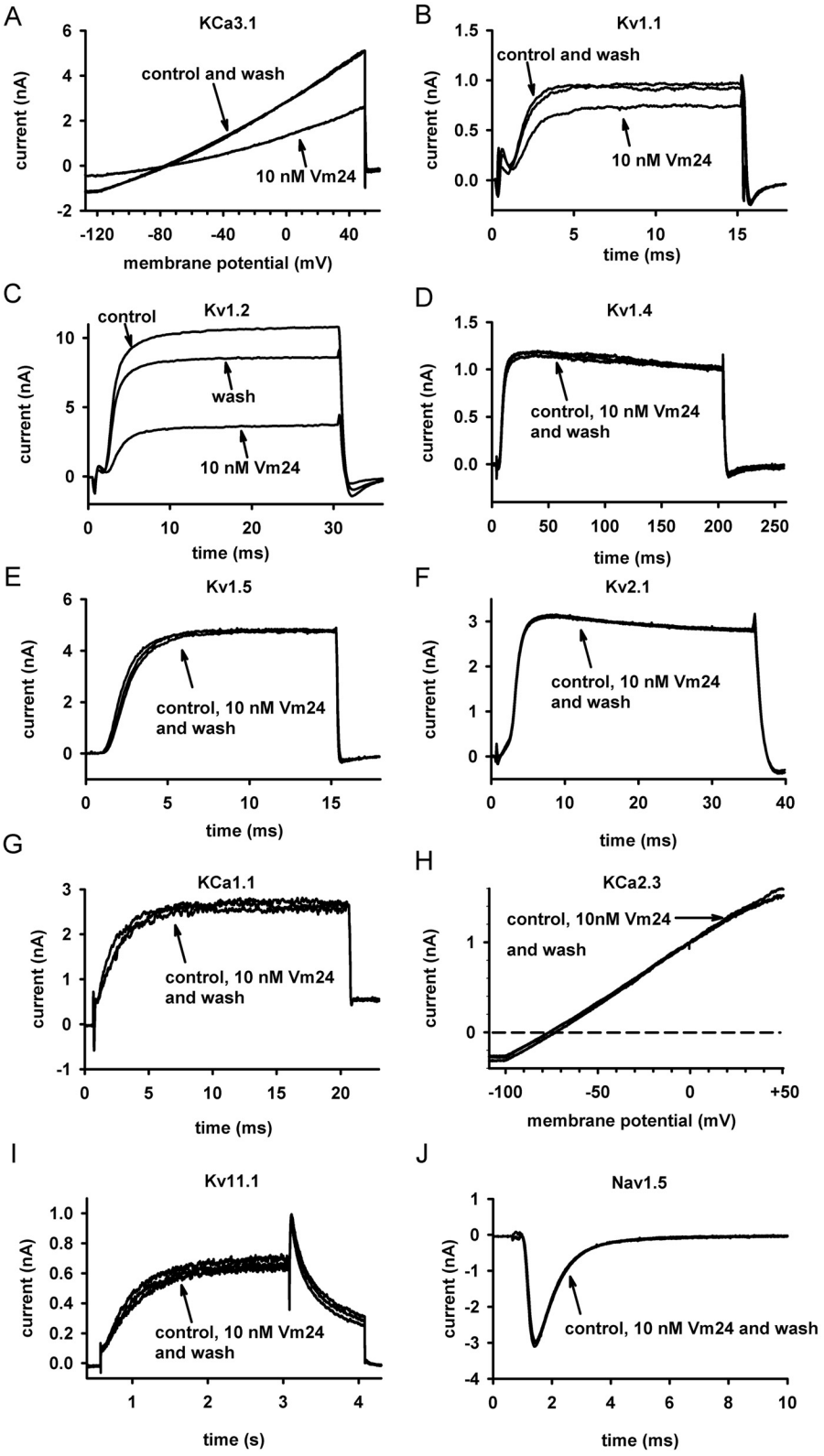

Fig. 4. Evidence that Vm24 has little or no effect on several ion channels. Current traces recorded before the application of the toxin (control), after equilibration of block by 10 nM Vm24, and after wash out (wash) of the toxin are shown for the following channels: hKCa3.1 (hIKCa1; Ca^{2+}-activated K^+ channels of T lymphocytes) (A), mKv1.1 (B), hKv1.2 (C), fast inactivation-removed hKv1.4 (Kv1.4ΔN) (D), hKv1.5 (E), rKv2.1 (F), KCa1.1 (hBK) (G), hKCa2.3 (hSK) (H), hKv11.1 (hERG) (I), and Nav1.5 (J) (for details on the expression systems, solutions, and voltage protocols, see *Materials and Methods*).

swelling of the challenged ear. Adoptive DTH was evoked with transfer of in vitro-activated Ova-GFP T lymphocytes into the animals, followed by ovalbumin challenge. The treatment group of animals received a single dose of 0.1 mg/kg Vm24 subcutaneously at the time of the challenge, whereas control animals received a PBS injection. The extent of the DTH reaction was evaluated 24 h later by measuring the specific ear swelling (change in ear thickness), as described under *Materials and Methods*. Figure 7 shows that a single dose of Vm24 significantly decreased the DTH response, to ~35 or 65% of the treatment control values for active and adoptive DTH, respectively. This result can be taken as a

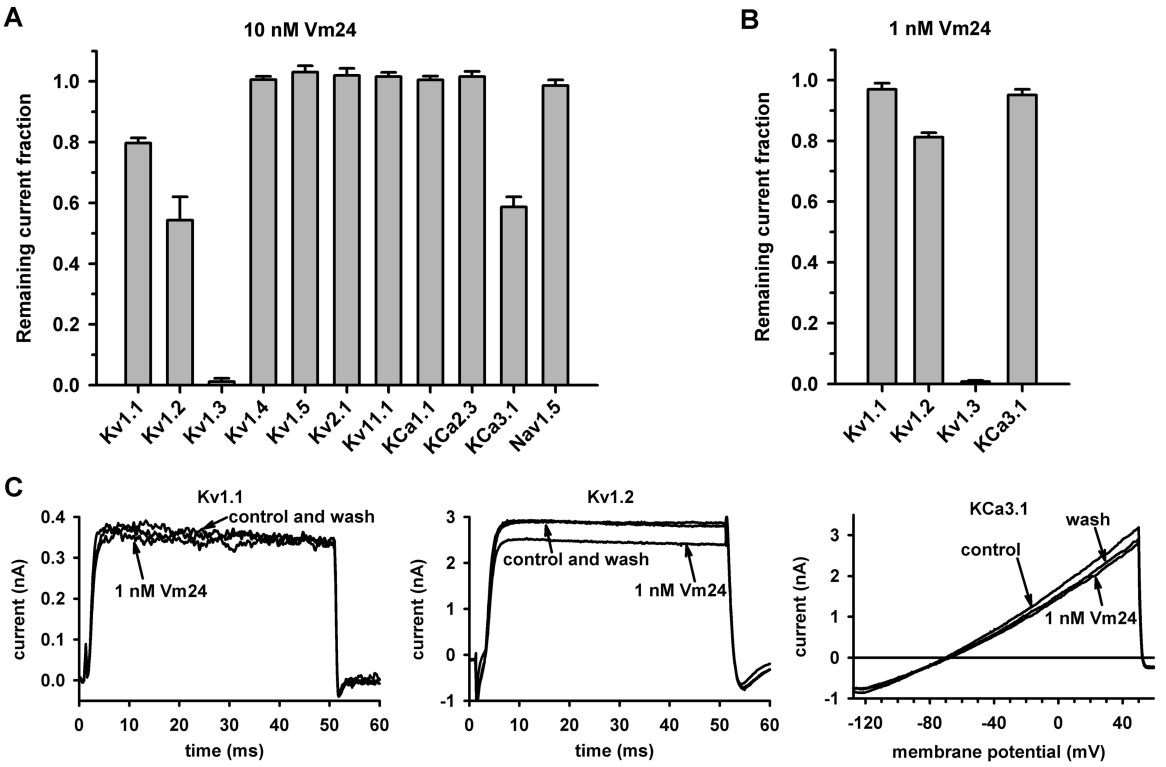

Fig. 5. Vm24 selectivity for Kv1.3 channels. A, remaining current fractions for the indicated channels with equilibrium block by Vm24, applied at 10 nM. Data are presented as mean ± S.E.M. for three or more independent experiments. B, remaining current fractions for channels that were partially blocked with 10 nM toxin and were tested again with 1 nM Vm24. C, effects of 1 nM Vm24 on Kv1.1, Kv1.2, and KCa3.1 currents. Current traces recorded before the application of the toxin (control), after the equilibration of blockade by 1 nM Vm24, and after wash out (wash) of the toxin are indicated (for details on the expression systems, solutions, and voltage protocols, see *Materials and Methods*).

"proof of concept" that Vm24 works in vivo as an immunomodulatory agent.

Discussion

We characterized the in vitro pharmacological properties and some in vitro and in vivo immunological effects of Vm24, a 36-amino acid peptide isolated from the venom of *V. mexicanus smithi*. Vm24 [α-KTx 23.1 (Gurrola et al., 2012)] is a high-affinity blocker of Kv1.3 channels of human T cells, with an estimated K_d of 2.9 pM. The peptide exhibited at least 1500-fold selectivity for Kv1.3 over other ion channels tested. The application of picomolar concentrations of Vm24 inhibited the proliferation of normal human T lymphocytes in vitro. Vm24 also suppressed DTH reactions in rats in vivo, which underscores the therapeutic potential of Vm24 as an immunosuppressive agent.

The mechanism through which scorpion toxins block K^+ channels involves plugging the ion conduction pathway after binding to the extracellular vestibule of the channel (Goldstein and Miller, 1993). We argue that Vm24 blocks Kv1.3 in a similar manner, despite the slow incomplete reversal of the current reduction, on the basis of the following findings: 1) the rate of current loss (at high toxin concentrations) depended on the concentration of Vm24, being faster at higher toxin concentrations; 2) the leak current did not increase in the presence of the toxin, which indicates a lack of general membrane damage by Vm24; 3) Vm24 did not inhibit several other K^+ currents or inhibited them quickly and reversibly (see the description of the selectivity profile below), which argues very strongly against a nonspecific action of the toxin; and 4) simultaneous application of ChTx (a well known pore blocker of Kv1.3) and Vm24 showed competition between the two toxins for the same binding site, which was evident in the slowing of Vm24 blocking kinetics with increasing ChTx concentrations. Some of these arguments are discussed further below.

During the analysis of the blocking kinetics of the current (Fig. 1D), we estimated the molecular association rate constant, k_{on}, as the inverse of the time constant for the development of the block (i.e., $k_{on} \approx 1/\tau_{Vm24,in}$). This approach is valid for conditions in which the dissociation rate of the toxin, k_{off} ($k_{off} = 1/\tau_{out}$, with $\tau_{out} \sim 3800$ s) (Fig. 1C), is negligible, compared with $k_{on} \times$ [Vm24], the pseudo-first-order association rate constant. This condition is fulfilled at Vm24 concentrations at which the Kv1.3 current block developed within minutes. At higher Vm24 concentrations (above 300 pM), the development of the block is too fast to be resolved accurately, given the minimal intervals of 15 s between successive current recordings (Fig. 1B). The perfectly linear relationship between Vm24 concentrations and $1/\tau_{Vm24,in}$ values (in the concentration range between 10 and 300 pM) supports the validity of our approach (Fig. 1D). The k_{on} value of 9.55×10^7 M^{-1} s^{-1} determined with this relationship is higher than typical values reported for peptide-channel interactions (Park and Miller, 1992a,b; Giangiacomo et al., 1993; Mullmann et al., 1999) but is similar to the values determined for the ShK toxin (Middleton et al., 2003) and Pi2 (Péter et al., 2001), with picomolar affinities for Kv1.3.

The strongest argument for specific binding of Vm24 to the extracellular vestibule is the competition between ChTx and

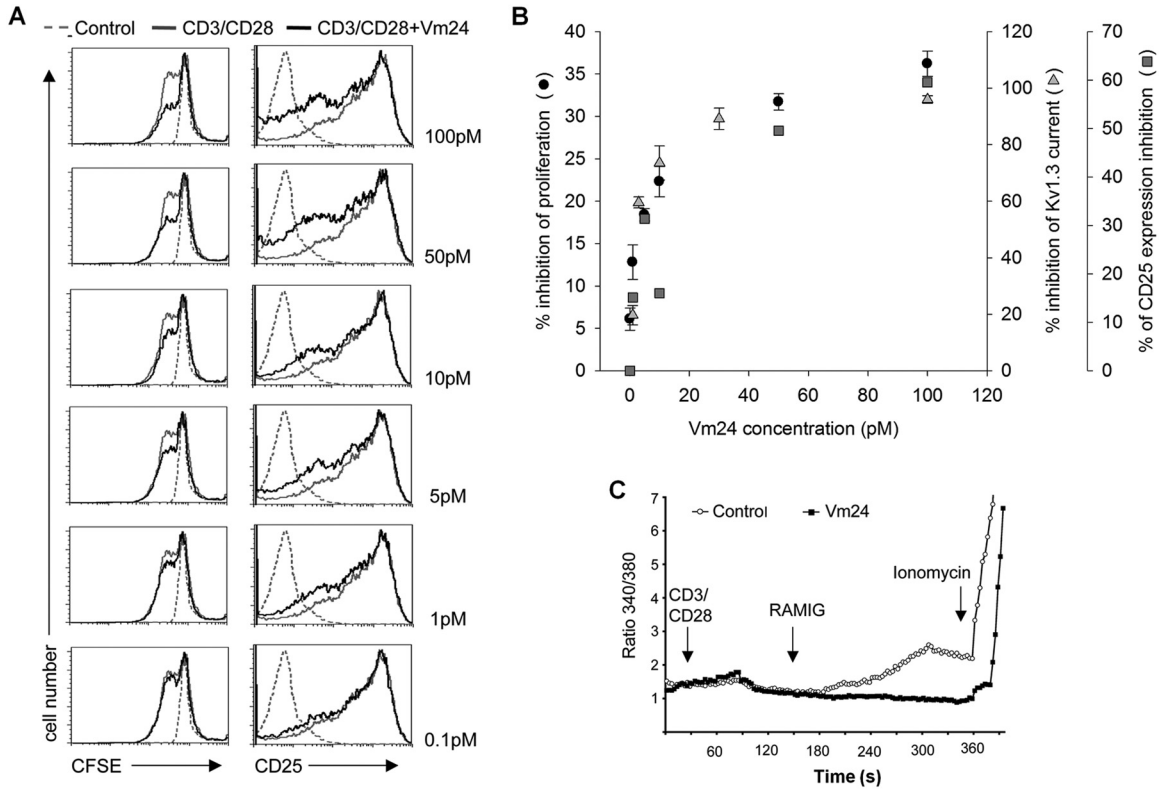

Fig. 6. In vitro effects of Vm24 on T-cell functions. A, effects on proliferation and CD25 expression. Left, CD3-CD28-induced proliferation was inhibited in the presence of Vm24. Resting human T lymphocytes were activated through cross-linking of CD3 and CD28, in the absence (CD3/CD28, gray histograms) or presence of the indicated doses of Vm24 (CD3/CD28+Vm24, black histograms). Cell proliferation was evaluated after 96 h through CFSE dilution. Dashed-line histograms (Control) show the CFSE level for cells left unstimulated for the duration of the experiment. Right, Vm24 controls CD25 expression. Purified resting human $CD4^+$ lymphocytes were activated by CD3 and CD28 engagement in the presence (CD3/CD28+Vm24, black histograms) or absence (CD3/CD28, gray histograms) of different doses of Vm24; after 24-h stimulation, the level of CD25 expression on the cell surface was measured with flow cytometry. Dashed-line histograms (Control) show the fluorescence of isotype control stained cells. Results are representative of at least three independent experiments. B, overlap between the dose-response relationships of the current inhibition (1 − RCF) and the inhibition of proliferation and CD25 expression. gray triangles, inhibition of Kv1.3 current; gray boxes, inhibition of CD25 expression; ●, inhibition of proliferation. C, Vm24 prevents CD3-CD28-dependent Ca^{2+} mobilization. Fura-2 ratios are shown for representative T cells. The calcium response of human peripheral blood T cells to CD3 and CD28 engagement was evaluated by using anti-CD3 and anti-CD38 antibodies and rabbit anti-mouse IgG (RaMIG) in a crosslinking system, in the absence (Control, gray) or presence 10 nM Vm24 (black). At the end of the experiment, the calcium ionophore ionomycin was applied as a positive control. Results are representative of at least three independent experiments.

Vm24 for the same or overlapping binding sites on Kv1.3. This strategy was used to show mutually exclusive binding of tetraethyl ammonium and ChTx to the pore of Shaker K^+ channels (Goldstein and Miller, 1993). The strong linear dependence of $1/\tau_{in,Vm24}$ (see above) on the fraction of channels not blocked by ChTx ($r^2 = 0.967$) supports our conclusion regarding the mutually exclusive binding of Vm24 and ChTx to the pore of Kv1.3 (Fig. 2C).

The very slow onset and relief of the Kv1.3 current inhibition made it difficult to determine the extent of equilibrium for Vm24, which imposed limitations on the determination of the equilibrium dissociation constant (K_d) (Fig. 3). Although the estimated k_{on} value was very high ($k_{on} = 9.55 \times 10^7\ M^{-1}\ s^{-1}$) (Fig. 1D), the extremely low peptide concentrations made the pseudo-first-order rate constant ($k_{on} \times$ [Vm24]) very small. For example, with a Vm24 concentration of 3 pM and the very slow off-rate, the time constant for reaching equilibrium block would be ~30 min. Therefore, the slow wash-out kinetics and the possibility of the rundown of the peak currents led to the use of an operational equilibrium block (see *Materials and Methods*) as the peak current at which consecutive pulses in the presence of the toxin caused negligible current decreases (less than 2%). The data presented in Fig. 3 represent the upper limits for I/I_0 values; therefore, the K_d value estimated from the dose-response relationship is also an overestimate of the real K_d (Péter et al., 2001). The k_{off}/k_{on} ratio yields a K_d value of 2.75 pM, which is in a good agreement with the value determined from the dose-response relationship. This indicates that the overestimation of the K_d value from the dose-response relationship was negligible, although the assumptions used to obtain k_{on} and k_{off} should be considered. The slow onset of the block and the consequent inaccurate determination of the equilibrium block have resulted in the significant discrepancy between the K_d values reported for the inhibition of Kv1.3 by ShK (Middleton et al., 2003).

Vm24 is similar to other natural peptides described in the literature with respect to its high-affinity block of Kv1.3 channels. Among these peptides, the affinities of ShK [estimated IC_{50} of 0.9 pM (Middleton et al., 2003) or 11 pM (Kalman et al., 1998)], OSK1 [α-KTx3.7, K_d = 14 pM (Mouhat et al., 2005)], HgTx1 [α-KTx2.5, K_d = 86 pM (Koschak et al., 1998)], MgTx [α-KTx2.2, K_d = 50 pM (Garcia-Calvo et al., 1993)], and HsTx1 [α-KTx6.3, K_d = 12 pM (Lebrun et al., 1997)] for Kv1.3 are remarkable. However, these peptides are all less selective for Kv1.3 than is Vm24; some of the peptides

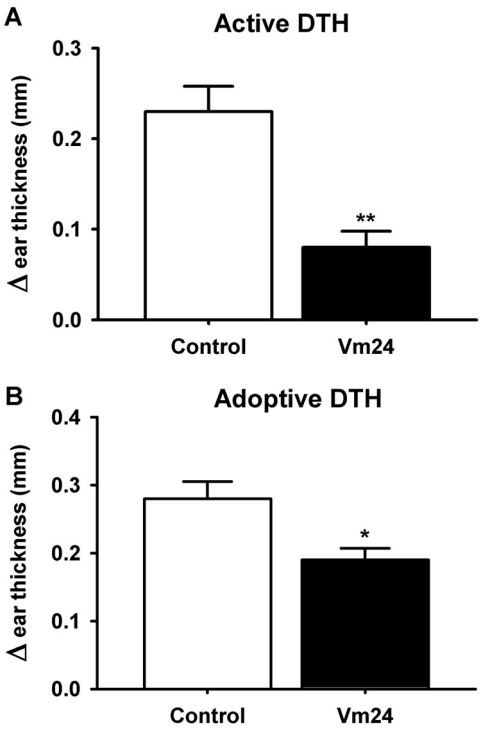

Fig. 7. Vm24 inhibition of DTH reactions in rats. Data are shown as differences in ear thickness between the ovalbumin-challenged left ear and the saline-treated right ear (mean ± S.E.M.). The treatment group of animals received a single dose of 0.1 mg/kg Vm24 administered subcutaneously at the time of the challenge, whereas the control group received the vehicle (PBS plus 2% rat serum). A, Vm24 inhibits active DTH directed against ovalbumin (n = 7 rats per group). **, $p \leq 0.01$. B, Vm24 inhibits adoptive DTH induced with Kv1.3^{high}-activated Ova-GFP T lymphocytes (n = 9 rats per group). *, $p \leq 0.05$.

(ShK, HgTx1, and MgTx) have similar or even higher affinities for Kv1.1, compared with Kv1.3, whereas others are selective for Kv1.3 but to a lesser extent than Vm24 (43- and 636-fold for OSK1 and HsTx1, respectively). The selectivity of Vm24 for Kv1.3 over other ion channels tested is at least 1500-fold, on the basis of the K_d value obtained from the dose-response relationship and the single-concentration estimates of the K_d values for the channels that were inhibited by Vm24. This value is well over the commonly accepted criterion for selectivity, which is defined as a 100-fold difference in the equilibrium dissociation constants for α-KTx binding to two different potassium channels (Giangiacomo et al., 2004). The ion channels that were inhibited with 10 nM Vm24 were Kv1.1, Kv1.2, and KCa3.1, whereas other tested channels were practically resistant to Vm24. It is noteworthy that 10 nM Vm24 is a >3000-fold higher concentration than the overestimated K_d for Kv1.3. Data presented in Fig. 5 indicated that the order of blocking potency of Vm24 for various ion channels was hKv1.3 ≫ hKv1.2 > hKCa3.1 > mKv1.1 ≫ hKv1.4 ≈ hKv1.5 ≈ rKv2.1 ≈ hKv11.1 ≈ hKCa1.1 ≈ hKCa2.3 ≈ hNa$_V$1.5. The >1500-fold selectivity of Vm24 was significantly better than the Kv1.3 selectivity achieved with recombinant mutant peptide toxins such as various OSK1 mutants, e.g., [Lys16,Asp20]-OSK1 (Mouhat et al., 2005), [Arg11,Thr28,His33]-BmKTx (Han et al., 2008), and ShK(L192) (Pennington et al., 2009), for which toxin selectivity ranged between 9- and 340-fold.

Key features of high-affinity Kv1.3 inhibitors are that they interfere with T-cell receptor activation-induced Ca^{2+} signaling and subsequent cell proliferation (Cahalan and Chandy, 2009). These characteristic features are clearly demonstrated for Vm24 in this study. Vm24, at concentrations overlapping with the block of the Kv1.3 current, inhibited CD3-CD28 ligation-induced T-cell proliferation and expression of the high-affinity interleukin-2 receptor α. Because Kv1.3 is the dominant K^+ channel of resting T cells of either subset (i.e., naive or T_{EM} cells), their proliferation is sensitive to Kv1.3 inhibition (Wulff et al., 2003). However, the inhibition of proliferation is not complete (in the case of Vm24 as well), even at peptide concentrations that fully inhibit Kv1.3 (Wulff et al., 2003; Hu et al., 2007). This may be an indication of the presence of other K^+ channel types in these cells (Meuth et al., 2008). A more-appropriate and widely used Kv1.3 inhibition-specific immunological test is the inhibition of DTH in rats (Beeton et al., 2006). The proliferation of T_{EM} cells responsible for DTH is persistently inhibited by highly selective Kv1.3 inhibitors, which results in decreased DTH responses. The potency of Vm24 to reduce DTH is similar to that of other peptides, such as ShK 192 (Pennington et al., 2009); a single dose of 0.1 mg/kg Vm24 efficiently inhibited both active and adoptive DTH. In general, the biological activity of Vm24 in vitro at the cellular level (proliferation and Ca^{2+} signaling) and in vivo resembles that of other high-affinity, high-selectivity Kv1.3 inhibitors.

The unique primary structure and the extremely high affinity and selectivity of Vm24 for Kv1.3 make this natural peptide an ideal tool to suppress T_{EM} cell-dependent immunological reactions in vivo, without significant side effects involving general immunosuppression. This confers a therapeutic potential to Vm24 for T_{EM} cell-dependent human autoimmune diseases such as multiple sclerosis, rheumatoid arthritis, and psoriasis.

Acknowledgments

We thank Cecilia Nagy and Erika Melchy for technical support.

Authorship Contributions

Participated in research design: Gurrola-Briones, Rodríguez de la Vega, Gaspar, Rosenstein, Beeton, Possani, and Panyi.

Conducted experiments: Varga, Gurrola-Briones, Papp, Pedraza-Alva, Tajhya, and Cardenas.

Performed data analysis: Varga, Gurrola-Briones, Papp, Pedraza-Alva, Tajhya, Gaspar, Cardenas, Rosenstein, Beeton, Possani, and Panyi.

Wrote or contributed to the writing of the manuscript: Varga, Rodríguez de la Vega, Rosenstein, Beeton, Possani, and Panyi.

References

Avdonin V, Tang XD, and Hoshi T (2003) Stimulatory action of internal protons on Slo1 BK channels. *Biophys J* **84:**2969–2980.

Bagdány M, Batista CV, Valdez-Cruz NA, Somodi S, Rodriguez de la Vega RC, Licea AF, Varga Z, Gáspár R, Possani LD, and Panyi G (2005) Anuroctoxin, a new scorpion toxin of the α-KTx 6 subfamily, is highly selective for Kv1.3 over IKCa1 ion channels of human T lymphocytes. *Mol Pharmacol* **67:**1034–1044.

Batista CV, Román-González SA, Salas-Castillo SP, Zamudio FZ, Gómez-Lagunas F, and Possani LD (2007) Proteomic analysis of the venom from the scorpion *Tityus stigmurus*: biochemical and physiological comparison with other *Tityus* species. *Comp Biochem Physiol C Toxicol Pharmacol* **146:**147–157.

Beeton C and Chandy KG (2007a) Induction and monitoring of active delayed type hypersensitivity (DTH) in rats. *J Vis Exp* **(6):**237.

Beeton C and Chandy KG (2007b) Induction and monitoring of adoptive delayed-type hypersensitivity in rats. *J Vis Exp* **(8):**325.

Beeton C, Wulff H, Standifer NE, Azam P, Mullen KM, Pennington MW, Kolski-Andreaco A, Wei E, Grino A, Counts DR, et al. (2006) Kv1.3 channels are a

therapeutic target for T cell-mediated autoimmune diseases. *Proc Natl Acad Sci USA* **103:**17414–17419.
Cahalan MD and Chandy KG (2009) The functional network of ion channels in T lymphocytes. *Immunol Rev* **231:**59–87.
Corzo G, Papp F, Varga Z, Barraza O, Espino-Solis PG, Rodríguez de la Vega RC, Gaspar R, Panyi G, and Possani LD (2008) A selective blocker of Kv1.2 and Kv1.3 potassium channels from the venom of the scorpion *Centruroides suffusus suffusus*. *Biochem Pharmacol* **76:**1142–1154.
Dauplais M, Lecoq A, Song J, Cotton J, Jamin N, Gilquin B, Roumestand C, Vita C, de Medeiros CL, Rowan EG, et al. (1997) On the convergent evolution of animal toxins. Conservation of a diad of functional residues in potassium channel-blocking toxins with unrelated structures. *J Biol Chem* **272:**4302–4309.
Estes DJ, Memarsadeghi S, Lundy SK, Marti F, Mikol DD, Fox DA, and Mayer M (2008) High-throughput profiling of ion channel activity in primary human lymphocytes. *Anal Chem* **80:**3728–3735.
Fierro NA, Pedraza-Alva G, and Rosenstein Y (2006) TCR-dependent cell response is modulated by the timing of CD43 engagement. *J Immunol* **176:**7346–7353.
Garcia-Calvo M, Leonard RJ, Novick J, Stevens SP, Schmalhofer W, Kaczorowski GJ, and Garcia ML (1993) Purification, characterization, and biosynthesis of margatoxin, a component of *Centruroides margaritatus* venom that selectively inhibits voltage-dependent potassium channels. *J Biol Chem* **268:**18866–18874.
Ghanshani S, Wulff H, Miller MJ, Rohm H, Neben A, Gutman GA, Cahalan MD, and Chandy KG (2000) Up-regulation of the IKCa1 potassium channel during T-cell activation: molecular mechanism and functional consequences. *J Biol Chem* **275:**37137–37149.
Giangiacomo KM, Ceralde Y, and Mullmann TJ (2004) Molecular basis of alpha-KTx specificity. *Toxicon* **43:**877–886.
Giangiacomo KM, Sugg EE, Garcia-Calvo M, Leonard RJ, McManus OB, Kaczorowski GJ, and Garcia ML (1993) Synthetic charybdotoxin-iberiotoxin chimeric peptides define toxin binding sites on calcium-activated and voltage-dependent potassium channels. *Biochemistry* **32:**2363–2370.
Goldstein SA and Miller C (1993) Mechanism of charybdotoxin block of a voltage-gated K^+ channel. *Biophys J* **65:**1613–1619.
Grissmer S, Nguyen AN, Aiyar J, Hanson DC, Mather RJ, Gutman GA, Karmilowicz MJ, Auperin DD, and Chandy KG (1994) Pharmacological characterization of five cloned voltage-gated K^+ channels, types Kv1.1, 1.2, 1.3, 1.5, and 3.1, stably expressed in mammalian cell lines. *Mol Pharmacol* **45:**1227–1234.
Grissmer S, Nguyen AN, and Cahalan MD (1993) Calcium-activated potassium channels in resting and activated human T lymphocytes: expression levels, calcium dependence, ion selectivity, and pharmacology. *J Gen Physiol* **102:**601–630.
Gurrola GB, Hernández-López RA, Rodríguez de la Vega RC, Varga Z, Batista CV, Salas-Castillo SP, Panyi G, et al. (2012) Structure, function, and chemical synthesis of *Vaejovis mexicanus* peptide 24: a novel potent blocker of Kv1.3 potassium channels of human T lymphocytes. *Biochemistry* **51:**4049–4061.
Han S, Yi H, Yin SJ, Chen ZY, Liu H, Cao ZJ, Wu YL, and Li WX (2008) Structural basis of a potent peptide inhibitor designed for Kv1.3 channel, a therapeutic target of autoimmune disease. *J Biol Chem* **283:**19058–19065.
Hu L, Pennington M, Jiang Q, Whartenby KA, and Calabresi PA (2007) Characterization of the functional properties of the voltage-gated potassium channel Kv1.3 in human $CD4^+$ T lymphocytes. *J Immunol* **179:**4563–4570.
Kalman K, Pennington MW, Lanigan MD, Nguyen A, Rauer H, Mahnir V, Paschetto K, Kem WR, Grissmer S, Gutman GA, et al. (1998) ShK-Dap22, a potent Kv1.3-specific immunosuppressive polypeptide. *J Biol Chem* **273:**32697–32707.
Koch RO, Wanner SG, Koschak A, Hanner M, Schwarzer C, Kaczorowski GJ, Slaughter RS, Garcia ML, and Knaus HG (1997) Complex subunit assembly of neuronal voltage-gated K^+ channels: basis for high-affinity toxin interactions and pharmacology. *J Biol Chem* **272:**27577–27581.
Koschak A, Bugianesi RM, Mitterdorfer J, Kaczorowski GJ, Garcia ML, and Knaus HG (1998) Subunit composition of brain voltage-gated potassium channels determined by hongotoxin-1, a novel peptide derived from *Centruroides limbatus* venom. *J Biol Chem* **273:**2639–2644.
Lebrun B, Romi-Lebrun R, Martin-Eauclaire MF, Yasuda A, Ishiguro M, Oyama Y, Pongs O, and Nakajima T (1997) A four-disulphide-bridged toxin, with high affinity towards voltage-gated K^+ channels, isolated from *Heterometrus spinnifer* (Scorpionidae) venom. *Biochem J* **328:**321–327.
Leonard RJ, Garcia ML, Slaughter RS, and Reuben JP (1992) Selective blockers of voltage-gated K^+ channels depolarize human T lymphocytes: mechanism of the antiproliferative effect of charybdotoxin. *Proc Natl Acad Sci USA* **89:**10094–10098.
Lewis RS (2001) Calcium signaling mechanisms in T lymphocytes. *Annu Rev Immunol* **19:**497–521.
Lin CS, Boltz RC, Blake JT, Nguyen M, Talento A, Fischer PA, Springer MS, Sigal NH, Slaughter RS, and Garcia ML (1993) Voltage-gated potassium channels regulate calcium-dependent pathways involved in human T lymphocyte activation. *J Exp Med* **177:**637–645.
Matteson DR and Deutsch C (1984) K channels in T lymphocytes: a patch clamp study using monoclonal antibody adhesion. *Nature* **307:**468–471.
Meuth SG, Bittner S, Meuth P, Simon OJ, Budde T, and Wiendl H (2008) TWIK-related acid-sensitive K^+ channel 1 (TASK1) and TASK3 critically influence T lymphocyte effector functions. *J Biol Chem* **283:**14559–14570.
Middleton RE, Sanchez M, Linde AR, Bugianesi RM, Dai G, Felix JP, Koprak SL, Staruch MJ, Bruguera M, Cox R, et al. (2003) Substitution of a single residue in *Stichodactyla helianthus* peptide, ShK-Dap22, reveals a novel pharmacological profile. *Biochemistry* **42:**13698–13707.
Mouhat S, Visan V, Ananthakrishnan S, Wulff H, Andreotti N, Grissmer S, Darbon H, De Waard M, and Sabatier JM (2005) K^+ channel types targeted by synthetic OSK1, a toxin from *Orthochirus scrobiculosus* scorpion venom. *Biochem J* **385:**95–104.
Mullmann TJ, Munujos P, Garcia ML, and Giangiacomo KM (1999) Electrostatic mutations in iberiotoxin as a unique tool for probing the electrostatic structure of the Maxi-K channel outer vestibule. *Biochemistry* **38:**2395–2402.
Muul LM, Silvin C, James SP, and Candotti F (2008) Measurement of proliferative responses of cultured lymphocytes. *Curr Protoc Immunol* **Chapter 7:**7.10.1–7.10.24.
Panyi G, Possani LD, Rodríguez de la Vega RC, Gáspár R, and Varga Z (2006) K^+ channel blockers: novel tools to inhibit T cell activation leading to specific immunosuppression. *Curr Pharm Des* **12:**2199–2220.
Panyi G, Varga Z, and Gáspár R (2004) Ion channels and lymphocyte activation. *Immunol Lett* **92:**55–66.
Park CS and Miller C (1992a) Interaction of charybdotoxin with permeant ions inside the pore of a K^+ channel. *Neuron* **9:**307–313.
Park CS and Miller C (1992b) Mapping function to structure in a channel-blocking peptide: electrostatic mutants of charybdotoxin. *Biochemistry* **31:**7749–7755.
Pennington MW, Beeton C, Galea CA, Smith BJ, Chi V, Monaghan KP, Garcia A, Rangaraju S, Giuffrida A, Plank D, et al. (2009) Engineering a stable and selective peptide blocker of the Kv1.3 channel in T lymphocytes. *Mol Pharmacol* **75:**762–773.
Péter M Jr, Varga Z, Hajdu P, Gáspár R Jr, Damjanovich S, Horjales E, Possani LD, and Panyi G (2001) Effects of toxins Pi2 and Pi3 on human T lymphocyte Kv1.3 channels: the role of Glu7 and Lys24. *J Membr Biol* **179:**13–25.
Soler D, Humphreys TL, Spinola SM, and Campbell JJ (2003) CCR4 versus CCR10 in human cutaneous TH lymphocyte trafficking. *Blood* **101:**1677–1682.
Wulff H, Calabresi PA, Allie R, Yun S, Pennington M, Beeton C, and Chandy KG (2003) The voltage-gated Kv1.3 K^+ channel in effector memory T cells as new target for MS. *J Clin Invest* **111:**1703–1713.
Wulff H, Gutman GA, Cahalan MD, and Chandy KG (2001) Delineation of the clotrimazole/TRAM-34 binding site on the intermediate conductance calcium-activated potassium channel, IKCa1. *J Biol Chem* **276:**32040–32045.

Address correspondence to: Gyorgy Panyi, Department of Biophysics and Cell Biology, Medical and Health Science Center, University of Debrecen, Nagyerdei krt. 98, Debrecen 4032, Hungary. E-mail: panyi@med.unideb.hu